



ISSN NO. 2320-5407

Journal Homepage: -www.journalijar.com

INTERNATIONAL JOURNAL OF ADVANCED RESEARCH (IJAR)

Article DOI:10.21474/IJAR01/3478
DOI URL: <http://dx.doi.org/10.21474/IJAR01/3478>



INTERNATIONAL JOURNAL OF
ADVANCED RESEARCH (IJAR)
ISSN 2320-5407
Journal homepage: <http://www.journalijar.com>
Journal DOI:10.21474/IJAR01

RESEARCH ARTICLE

EFFECT OF HEATING RATES AND Zn-ADDITION ON THE THERMAL PROPERTIES OF Pb–Sn ALLOY

*Ali Alnakhilani¹, Belqees Hassan¹, Abdulhafiz Muhammad² and Muhammad Ali Al-Hajji³.

1. Faculty of Sciences, Department of Physics, Ibb University, Ibb, Yemen.
2. Faculty of Sciences, Department of Physics, Damascus University, Syria.
3. Faculty of civil engineering, Department of basic science, Damascus University, Syria.

Manuscript Info

Manuscript History

Received: 06 January 2017
Final Accepted: 08 February 2017
Published: March 2017

Key words:-

Thermal properties; Differential Thermal Analysis (DTA); Enthalpy of fusion; Activation energy.

Abstract

The variations of thermal properties with temperature for Pb–Sn alloys were measured using a heat flow apparatus. According to present experimental results, the thermal parameters (T_{onset} , T_{end} , T_m) of Pb–Sn alloys increase with increasing heating rates, also the results showed that the small amount of zinc improved significantly these parameters. Furthermore the change in enthalpy of fusion and activation energy of fusion for different heating rates were studied experimentally by the differential thermal analysis (DTA). The apparent activation energies of Pb–Sn alloys have been determined based on the Kissinger equation.

Copy Right, IJAR, 2017.. All rights reserved.

Introduction:-

Pb–Sn alloys are the basis of many engineering materials [1]. An Extensive theoretical and experimental study of the nature of the relationships among microstructure, physical properties and solidification processing parameters has been created [2-5]. Pb–Sn solders are one of the most familiar materials used for various microelectronic connections in computer industry. Different compositions of Pb–Sn solders have considerable potential for advanced structural and electronic applications. Pb–Sn alloys have several attractive attributes: low cost, low eutectic temperature (183°C), good wettability on many common workpiece metals, and good thermal and electrical conductivities, and a choice between eutectic freezing or a wide freezing range which produces “pasty” solid–liquid mixtures[5-8]. Also, a great deal of efforts has been carried out on Pb–Sn eutectic alloys, which is currently used in computer industry for various microelectronic connections [9-12]. Although Pb–Sn solders are still widely used for many applications (e.g., body panel soldering on automobiles). Pb–Sn alloys make excellent solders for electrical and mechanical joining[13]. One of the important benefits of the thermal analysis experiment is its usefulness in selecting appropriate temperatures for the heat treatment cycles of the samples as well as for the investigation of the phase development[14, 15].

Most studies have dealt with the thermal properties of Pb–Sn solders with different compositions at room temperature, but a few papers have been focused on the dependency of thermal properties of these alloys on the temperature and composition of alloy. Thus, the purpose of present work was to determine the following parameters: temperature of onset of melting (T_{onset}), temperature of offset of melting (T_{offset}), heat of fusion, and the activation energy occurring during melting, besides the effects of different heating rates and Zn addition on melting temperature, heat of fusion, and the activation energy of the alloy samples.

Corresponding Author:-Ali Alnakhilani.

Address:-Department of Physics, Faculty of Sciences, Ibb University, Ibb, Yemen.

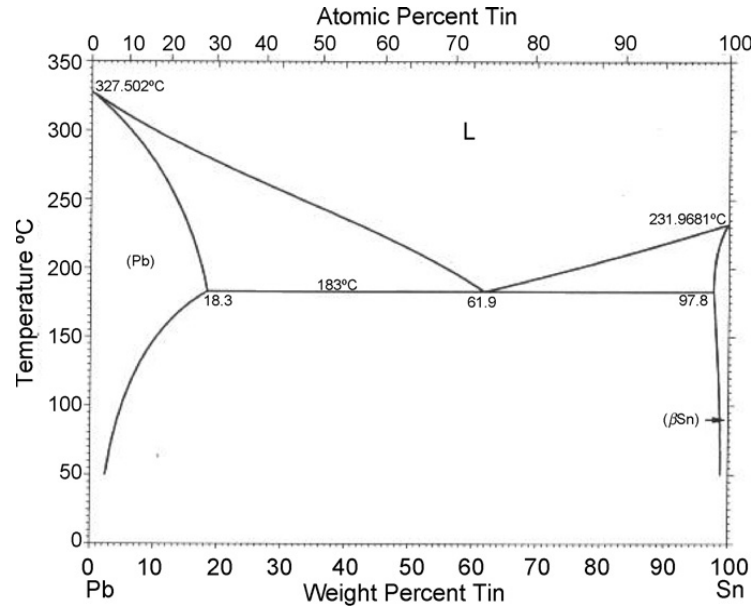


Figure 1:- Phase Diagram of Pb–Sn System

Phase diagram of Pb–Sn system has been evaluated as shown in Figure 1. Solubility of Pb in solid Sn and Sn in solid Pb at the eutectic temperature (456 K) are 2.2 wt.% Pb and 18.3 wt.% Pb, respectively [16]. Thus, the compositions of Pb–Sn alloys were chosen to be Pb–61.9 wt% Sn, Pb–61.9 wt% Sn-2 wt% Zn to investigate the dependence of the thermal measurements on the temperature and the effect of addition of Zn in the Pb–Sn alloys.

Experimental Details:-

Material Preparations:-

The two solder alloys, Pb-61.9wt%Sn and Pb-61.9wt%Sn-2wt% Zn were prepared from high purity Pb, Sn and Zn of purity 99.99%. The appropriate weights of the elements for the binary and ternary alloys were well mixed with CaCl_2 flux to prevent oxidation in a graphite mold. Casting in rod form was performed in a 15 x1 x 1 cm graphite mold. The casting rod was annealed at 438K for 50 hours. The ingots were rolled into wires of diameter 1mm. In this study, the samples were annealed at 443K for 4h and then slowly cooled to room temperature at cooling rate $T = 2 \times 10^{-2} \text{ Ks}^{-1}$.

Mechanical Tests:-

Differential thermal analysis (DTA) measurements were carried out on 40 mg of small pieces of alloy samples using a Labsys Evo_TG DTA thermal analyzer. DTA experiments were performed by heating the samples in a Pt crucible with Al_2O_3 as the reference material. Five different heating rates (10, 15, 20, 25 and 30 $^\circ\text{C min}^{-1}$) were examined during the measurements.

Results and Discussion:

Melting Temperature (T_m) of Alloys:-

The melting temperature is a critical alloy characteristic because it determines the maximum operating temperature of the system. Figure2 represents the results of DTA analysis of the Pb-61.9wt%Sn and Pb-61.9 wt%Sn-2wt%Zn alloys measured at the heating rates of 10, 15, 20, 25 and 30 $^\circ\text{C min}^{-1}$, from room temperature to 450 $^\circ\text{C}$.

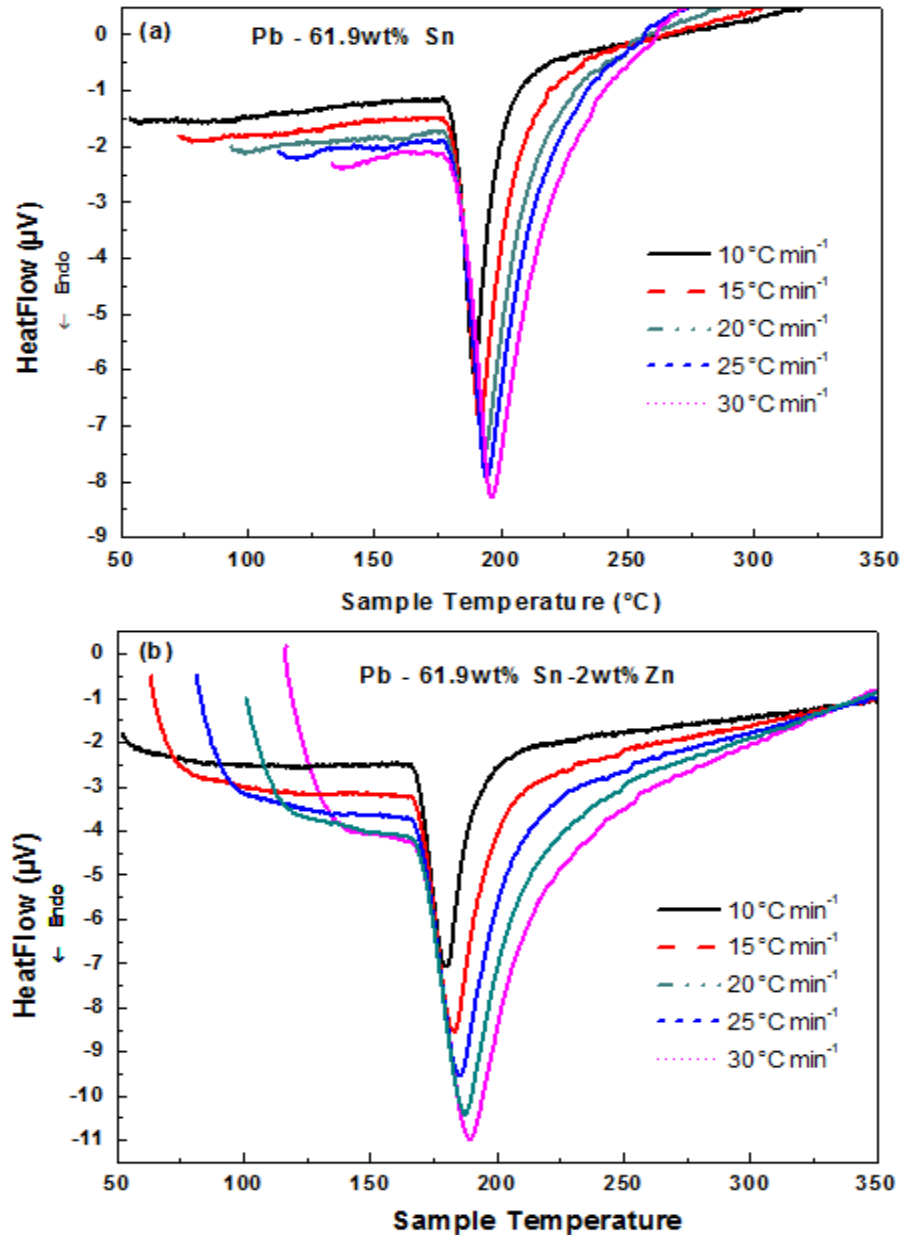


Figure 2:- Different Thermal Analysis (DTA) Curves for (a) Pb-61.9wt%Sn and (b) Pb-61.9 wt%Sn-2 wt% Zn Alloys Taken at Different Heating Rates.

It is shown that there is only one main endothermic peak for the samples during the measurements observed in the temperature range 30 – 450 °C, namely the melting which is indicated by the endothermic peak. The endothermic peak appears in DTA curve has two regions of heat extraction that are indicative of the melting temperature. The melting points were considered in support of probable industrial applications. The temperature of onset of melting, T_{onset} , (the onset point of heat absorption during heating) is defined by the extrapolated beginning of the curve, being defined by the point of intersection of the tangent with the point of maximum slope, on the principal side of the peak with the base line extrapolated [17, 18].

From Figure 2 (a, b) and Table 1, it can also be seen that the heating curves of the Pb-61.9wt%Sn and Pb-61.9 wt%Sn-2wt% Zn alloys are shifted towards higher temperature with the increasing rate of heating. The first effect of the heating rate can be explained by the decrease of the precipitated Zn atoms amount because of its increased solid

solubility at the increased precipitation temperatures when using higher heating rate [19, 20]. However the second effect is explained by the diffusive nature of the precipitation reactions.

Figure3 shows a schematic of the heat flow curve versus the temperature of Pb-61.9 wt%Sn-2 wt% Zn alloy obtained at the heating rate of $10\text{ }^{\circ}\text{C min}^{-1}$ and how the DTA curve is formed from the data recorded. The graph shows that the sample presents an onset temperature for melting of $169.809\text{ }^{\circ}\text{C}$ with $\Delta H= 8.425\text{ }(\mu\text{V.s/mg})$ and a melting temperature of $180.246\text{ }(^{\circ}\text{C})$.

The obtained values of the temperature of onset of melting (T_{onset}), the temperature of offset of melting (T_{offset} or T_{end}) and melting temperature (T_m) are listed in Table 1 and marked on the DTA curves as shown in Figure3 for Pb-61.9 wt%Sn-2 wt% Zn alloy obtained at a heating rate of $10\text{ }^{\circ}\text{C/min}$ (as example).

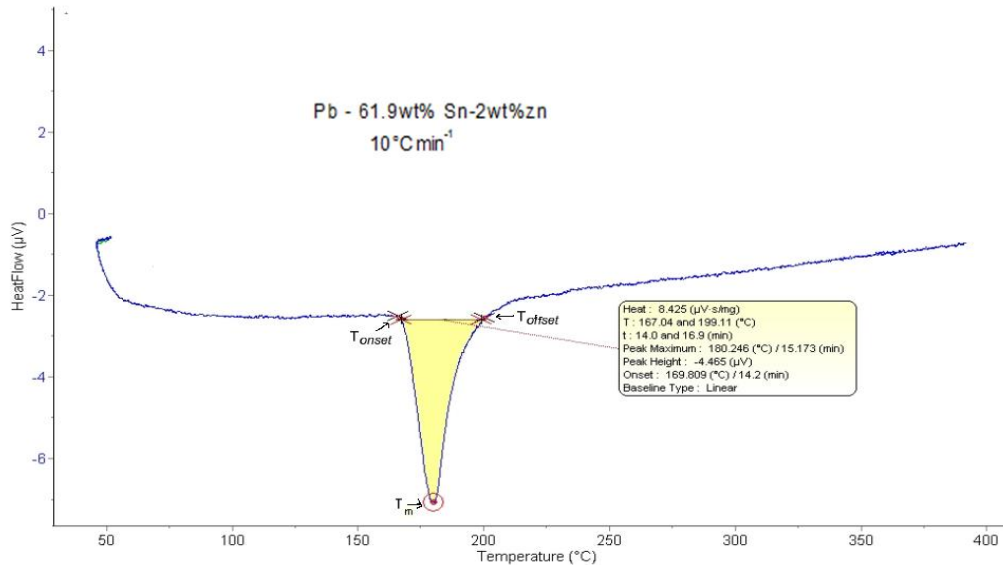


Figure 3:- Schematic of Heat Flow Curve Versus the Temperature for Pb-61.9 wt%Sn-2 wt% Zn Alloy at a Heating Rate of $10\text{ }^{\circ}\text{C/min}$.

Figure: 4 shows the comparison between the values of the melting temperature T_m for Pb-61.9 wt% Sn and Pb-61.9 wt%Sn-2 wt% Zn alloys at a heating rate of $10\text{ }^{\circ}\text{C/min}$. Addition of Zn increased the T_{onset} , and T_{end} as illustrated in Figure4 whereas, the Zn addition caused a further depressed of the melting temperature T_m of Pb-61.9wt%Sn alloy for different heating rate, which makes this alloy interesting for technical applications. In addition the melting range (temperature range between solidus and liquids points according to DTA) is extended as zinc metal addition.

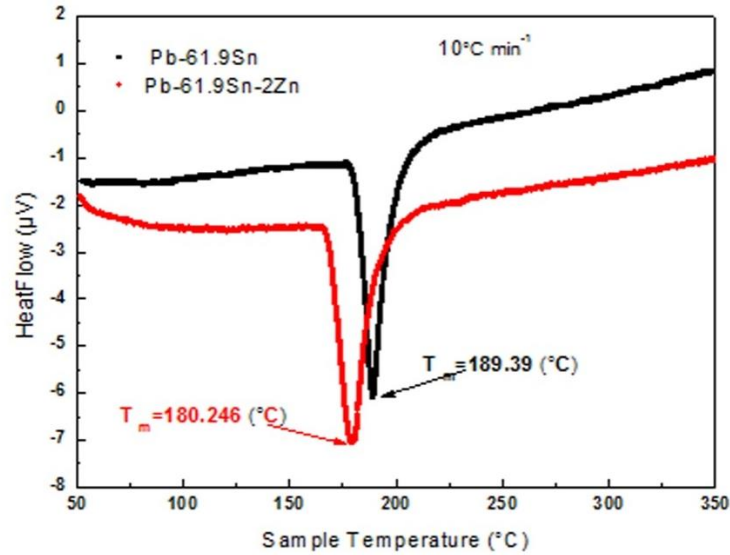


Figure 4:- Heat Flow Curve Versus the Temperature for Pb-61.9 wt% Sn and Pb-61.9 wt%Sn-2 wt% Zn Alloys at a Heating Rate of 10 °C/min.

Table 1:- Comparison of Onset Temperature (T_{onset}), Offset Temperature (T_{end}), Melting Temperature (T_m), and Heat of Fusion (ΔH) for Pb-61.9wt%Sn and Pb-61.9wt%Sn-2wt%Zn Alloys.

Alloys	Heating rate (°C min ⁻¹)	T_{onset} (°C)	T_{end} (°C)	T_m (°C)	ΔH (µV.s/mg)	E_a (kJmol ⁻¹)
Pb-61.9Sn	10	183.04	204.4	189.39	6.612	47.7
	15	182.569	212.3	191.66	6.494	
	20	183.787	217.7	193.489	6.204	
	25	183.67	220.4	194.216	5.637	
	30	184.935	224.9	196.269	5.676	
Pb-61.9Sn-2Zn	10	169.809	193.4	180.246	8.425	31.5
	15	170.896	205.1	183.366	7.728	
	20	170.844	211.2	185.343	7.396	
	25	172.07	219.9	187.344	7.673	
	30	171.611	225.6	189.422	8.031	

Determination of activation energy (E_a) of fusion:-

To determine the activation energy E_a for fusion of alloys by Kissinger methods, which determine the activation energy of the samples starting from the change in the temperature that corresponds to the maximum of the endothermic peak T_m according to the heating rate β as shown in Figure2 (a,b).

The activation energy of the Pb-61.9wt%Sn and Pb-61.9 wt%Sn-2wt%Zn alloys under continuous heating condition can be calculated by the Kissinger equation[21-23]:

$$\ln \left[\frac{\beta}{T_m^2} \right] = -\frac{E}{RT_m} + C, \quad (1)$$

Or it can be written as

$$\frac{d \ln \left(\frac{\beta}{T_m^2} \right)}{d \left(\frac{1}{T_m} \right)} = -\frac{E_a}{R} + C, \quad (2)$$

Where β is the heating rate, E_a is the activation energy of fusion and R is the gas constant (8.314J/mol K), T_m denotes the maximum melting endothermic peak, and C is a constant.

If the fusion mechanism remains constant with the heating rate (β), the plot of $\ln (\beta/T_m^2)$ vs. $1000/T_m$ gives a straight line and E_a is calculated from the slope of this line. Figure5 shows the Kissinger plot for the Pb-61.9Sn-2Zn alloy.

Table 1 lists the calculated activation energies for fusion. The calculated value of E_a decreased from 47.7 kJmol^{-1} for Pb-61.9wt%Sn alloy to 31.5 kJmol^{-1} for Pb-61.9 wt%Sn-2wt%Zn alloy. It is clear that a small amount of Zn-addition enhances the activation energies of fusion.

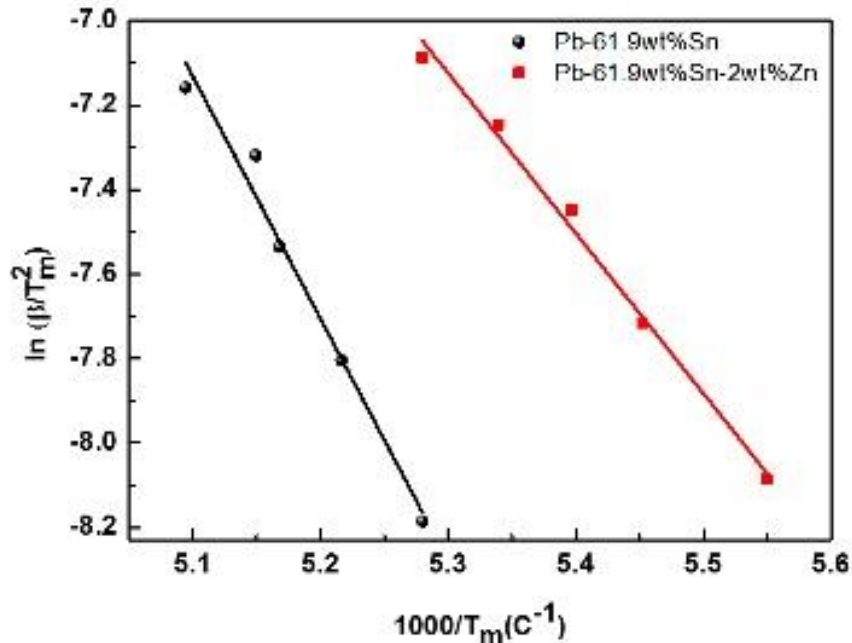


Figure 5:- Kissinger plot of Pb-61.9wt%Sn and Pb-61.9wt%Sn-2wt%Zn

Measuring the enthalpy and specific heat of fusion:-

The heat of fusion is calculated by integrating the area under the melting peak between the peaks start T_{onset} and end T_{end} temperatures. The heat of fusion, ΔC_p , can be determined by Eq. (3) for each material[24]:

$$\Delta C_p = \frac{KA}{m}, \quad (3)$$

Where K is a constant that depends on crucible shape and regards as a constant in the DAT system, m is the mass of the sample, and A is the area under the endothermic peak.

At the melting point, the heat supplied to system will be used supplying the enthalpy of fusion (latent heat of fusion) that is required to convert solid to liquid. Latent heat of fusion is the energy absorbed in a material during its phase change from solid to liquid. For a transformation from solid state to liquid state, enthalpy of fusion can be expressed as:

$$\Delta H \approx \Delta C_p T_m, \quad (4)$$

The enthalpy of fusion (ΔH) and the specific heat change (ΔC_p) were determined because of they are very important parameters for industrial applications. The values of T_{onset} , T_{end} , and ΔH for the two alloys are listed in Table 1. It is obvious that, the fusion heat of Pb-61.9wt%Sn-2wt%Zn is larger than that of the Pb-61.9wt%Sn alloy.

Summary and Conclusions:-

In this work, a detailed analysis of the effects of different heating rates and Zn addition on the melting temperature, heat of fusion, and the activation energy have been investigated. Both Zn addition and heating rates significantly affect the alloys behavior. DTA curves indicate that a small amount of Zn-addition enhances the transition temperature and also melting temperature decrease significantly.

The obtained data on the thermal properties measurements have shown an increase on T_{onset} , T_{end} and T_m values of the samples when the heating rates was increased. The maximum peak in Figure2 is shifted to the higher temperature with increasing heating rates.

In conclusion, this study demonstrated that the heating rate had a significant effect on the values obtained for alloy samples prepared, since the values of T_{onset} , T_{end} and T_m diminish as the heating rate increases. The results showed

that the addition of small amount Zn in Pb–Sn alloy leads to a decrease of thermal parameters (T_{onset} , T_{end} and T_m) and activation energy of fusion.

Acknowledgments:-

The authors would like to thank Damascus University in Syria for providing facilities and support to setup the testbed. This original research was proudly supported by Ibb University in Yemen.

Disclosure:-

The authors declare that there is no conflict of interest regarding the publication of this paper.

References:-

1. M. C. Flemings, "Solidification processing," *Metallurgical transactions*, vol. 5, pp. 2121-2134, 1974.
2. E. Çadırlı, H. Kaya, and M. Gündüz, "Directional solidification and characterization of the Cd–Sn eutectic alloy," *Journal of alloys and compounds*, vol. 431, pp. 171-179, 2007.
3. A. El-Daly, Y. Swilem, and A. Hammad, "Creep properties of Sn–Sb based lead-free solder alloys," *Journal of Alloys and Compounds*, vol. 471, pp. 98-104, 2009.
4. S. Guruswamy, *Engineering properties and applications of lead alloys*: CRC Press, 1999.
5. A. El-Daly, A. Abdel-Daiem, and M. Yousf, "Effect of isothermal ageing on the electrical resistivity and microstructure of Pb–Sn–Zn ternary alloys," *Materials chemistry and physics*, vol. 78, pp. 73-80, 2003.
6. Y. Ocak, S. Aksöz, N. Maraşlı, and E. Çadırlı, "Dependency of thermal and electrical conductivity on temperature and composition of Sn in Pb–Sn alloys," *Fluid Phase Equilibria*, vol. 295, pp. 60-67, 2010.
7. E. Çadırlı, U. Büyük, H. Kaya, N. Maraşlı, S. Aksöz, and Y. Ocak, "Dependence of electrical resistivity on temperature and Sn content in Pb–Sn solders," *Journal of electronic materials*, vol. 40, pp. 195-200, 2011.
8. Y. Plevachuk, V. Sklyarchuk, A. Yakymovych, B. Willers, and S. Eckert, "Electronic properties and viscosity of liquid Pb–Sn alloys," *Journal of alloys and compounds*, vol. 394, pp. 63-68, 2005.
9. M. Sakr, A. Mohamed, M. Shehab, and A. Bassyouni, "Microstructure changes and steady state creep characteristics in Pb–Sn alloys during transformation," *Czechoslovak journal of physics*, vol. 41, pp. 785-792, 1991.
10. C. Morando, O. Fornaro, O. Garbellini, and H. Palacio, "Thermal properties of Sn-based solder alloys," *Journal of Materials Science: Materials in Electronics*, vol. 25, pp. 3440-3447, 2014.
11. S. K. Kang and A. K. Sarkhel, "Lead (Pb)-free solders for electronic packaging," *Journal of Electronic Materials*, vol. 23, pp. 701-707, 1994.
12. I. Anderson, "Tin-silver-copper: A lead free solder for broad applications," in *NEPCON WEST*, 1996, pp. 882-890.
13. A. Russell and K. L. Lee, *Structure-property relations in nonferrous metals*: John Wiley & Sons, 2005.
14. P. Gong, X. Wang, and K. Yao, "Effects of alloying elements on crystallization kinetics of Ti–Zr–Be bulk metallic glass," *Journal of Materials Science*, vol. 51, pp. 5321-5329, 2016.
15. R. Fukahori, T. Nomura, C. Zhu, N. Sheng, N. Okinaka, and T. Akiyama, "Thermal analysis of Al–Si alloys as high-temperature phase-change material and their corrosion properties with ceramic materials," *Applied Energy*, vol. 163, pp. 1-8, 2016.
16. H. Baker and H. Okamoto, "Alloy phase diagrams," *ASM International, ASM Handbook.*, vol. 3, p. 501, 1992.
17. W. J. Boettinger, U. Kattner, K. Moon, and J. Perepezko, *DTA and heat-flux DSC measurements of alloy melting and freezing*: Citeseer, 2006.
18. Z. S. Šimšić, D. Živković, D. Manasijević, T. H. Grgurić, Y. Du, M. Gojić, *et al.*, "Thermal analysis and microstructural investigation of Cu-rich alloys in the Cu–Al–Ag system," *Journal of alloys and compounds*, vol. 612, pp. 486-492, 2014.
19. A. Varschavsky and E. Donoso, "A differential scanning calorimetric study of precipitation in Cu 2Be," *Thermochimica acta*, vol. 266, pp. 257-275, 1995.
20. E. Donoso and A. Varschavsky, "Microcalorimetric evaluation of precipitation in Cu–2Be–0.2 Mg," *Journal of thermal analysis and calorimetry*, vol. 63, pp. 249-266, 2001.
21. R. T. Yang and M. Steinberg, "Reaction kinetics and differential thermal analysis," *The Journal of Physical Chemistry*, vol. 80, pp. 965-968, 1976.
22. P. Altuzar and R. Valenzuela, "Avrami and Kissinger theories for crystallization of metallic amorphous alloys," *Materials letters*, vol. 11, pp. 101-104, 1991.

23. H. Lashgari, Z. Chen, X. Liao, D. Chu, M. Ferry, and S. Li, "Thermal stability, dynamic mechanical analysis and nanoindentation behavior of FeSiB (Cu) amorphous alloys," *Materials Science and Engineering: A*, vol. 626, pp. 480-499, 2015.
24. B. M, "Introduction to Thermal Analysis," *Wiley*, pp. 33-35, 1986.